Synergic use of altimeter and model sea level data in inner and coastal seas

Luigi Cavaleri [a,*], Luciana Bertotti [a], Christian Ferrarin [a], Marcello Passaro [b], Paolo Pezzutto [a], Angela Pomaro [a]

[a] Consiglio Nazionale delle Ricerche - Istituto di Scienze Marine (CNR-ISMAR), Arsenale - Tesa 104, Castello 2737F, 30122 Venezia, Italy
[b] Deutsches Geodatisches Forshungsinstitut, Technische Universitat Munchen (DGFITUM), Arcisstraβe 21, 80333 Munchen, Germany

ARTICLE INFO

ABSTRACT

We analyse high rate (20 Hz) altimeter derived sea level information, both from Synthetic Aperture Radar (SAR) altimetry missions and Low Resolution Mode missions, in an inner sea and coastal environment. They are compared versus measured and high resolution model data. After a compact description of the relevant physical processes affecting the local sea level values, we focus on three specific passes on the Adriatic Sea, East of Italy. Our main finding is that altimeters and models provide both valuable, partially overlapping, but complementary, information to be exploited in parallel with a double purpose: to progressively approach the truth and to ensure the parallel improvement of both sources. From altimeter data there is a very strong suggestion that the spatial, and implicitly temporal, variability of the fields is much higher than shown by models. The reasons are discussed.

1. Offshore and coastal altimetry

The launch of GEOSAT in 1985 and of ERS-1 in 1991 opened the still ongoing successful period of intensive use of altimeter data. Indeed, the almost real time availability of wave heights and, although with some delay, sea level data had been for a long while a dream of all mariners and oceanographers. The last three decades have seen a growing list of successes and ever-expanding fields of use. The abstracts of the presentations at the European Space Agency (ESA) Milan Symposium (see ESA, 2019) provide an effective list of the possible present applications. As usual, the focus of attention has been the timely measurement of sea level height η. Indeed, this information is fundamental for global circulation, at least on a large scale. One of the most spectacular measurements, when the altimeter happens to pass at the right time and location, is the detection of sea level rising (inverse barometer effect) at the centre of hurricanes or typhoons. Of course improvements are still possible, and new applications are constantly explored.

The significant wave height H_s is arguably one of the most important products from an engineering point of view, despite it originally being a by-product of the single measurements and not the main focus of attention. Along with the contribution of buoy data (Jensen et al., 2017) and of measurements from oil rigs (see, as an example, Donelan and Magnusson, 2017), satellite altimetry has provided an unprecedented volume of information on the open ocean. For a long while, the only source of information on the vast oceans had been the 3-hourly visual reports by ships travelling between two continents or countries (if in more coastal or enclosed seas, such as the Mediterranean Sea). Apart from the inherent approximations, these data had the basic problem of being unavoidably concentrated on the main navigation routes. On the other hand the abundant information of typical altimetry, distributed at one value per second (1 Hz data) and spanning the whole ocean surface, has provided more or less uniformly distributed information, limited only by the choice of the satellite orbital trajectory. Beside providing direct information, almost in real-time, to modelling and forecasting systems (see, e.g., Bidlot, 2019), these data have frequently opened the mind of wave oceanographers, revealing the existence of significant wave heights well beyond the supposed limits in the early '90s. After practically thirty years of cumulative information, Young and Ribal (2019) have been able to provide a reliable global wave statistics of the possible H_s, with also some information about long term trends.

Within this ocean wide perspective of significant wave height and sea level data, we should not forget that a large part of our interests lies on coastal data. The coast is where much of what we build has to withstand the sea force, and at the same time is where we tend to pack with a higher density. From an oceanographic perspective, this is also where hydraulic processes like tides, shallow water waves, ocean piling up against the coast because of wind stress and wave breaking, often have their largest values and, most of all, their largest time and spatial

* Corresponding author.
E-mail addresses: luigi.cavaleri@ismar.cnr.it (L. Cavaleri), luciana.bertotti@ismar.cnr.it (L. Bertotti), c.ferrarin@ismar.cnr.it (C. Ferrarin), marcello.passaro@tum.de (M. Passaro), pezzutto.paolo@gmail.com (P. Pezzutto), angela.pomaro@cnr.it (A. Pomaro).

gradients due to the rapidly shallowing waters towards the coast.

Aware of this strong requirement, the satellite community has reacted by improving the resolution of the altimeter data close to coast with the Synthetic Aperture Radar (SAR) mode of operation (also called Delay-Doppler altimeter) which is currently on board the Cryosat-2 and the Sentinel-3 A and B satellites (Vignudelli et al., 2019). While in the usual application each altimeter pulse explores a circular sea area a few kilometres wide whose extent depends on the wave conditions, in SAR mode we exploit the information of each 20 Hz pulse, exploring an area still a few kilometres wide in cross-flight direction, but only 300 m long in flight direction. If this is perpendicular to the coastline, this allows retrieving information much closer to coast before the presence of land disrupts the return signal. Of course, as in the classical ("Low Resolution Mode") altimeters, the price to pay when using "high frequency" 20 Hz data instead of the typical 1 Hz averages is a higher noise in the return signal because of the much reduced area sampled by each pulse. The precision of sea level retrievals from SAR altimetry is nevertheless higher (Passaro et al., 2016), and it should therefore ease the exploitation of the high frequency data.

Some of us have already discussed (Cavaleri et al., 2019a) the parallel problem of the reliability of significant wave height data in inner seas and coastal waters. In general, it is relatively common for an altimeter to come across areas, also close to the coast, where the significant wave height H_s has interesting, i.e. large, values, possibly also with large spatial gradients. In the latest years the development of improved fitting techniques (re-trackers) for the coastal zone succeeded in retrieving higher amounts of valid H_s (Passaro et al., 2015) and sea level data (Marti et al., 2019) closer to the coast, although usually the number of measurements that are clearly not outliers drops significantly in the last 3 km from the coast. A successful technique consists in using only a portion of the waveform in order to avoid considering spurious contribution in the circular pattern at nadir (Cipollini et al., 2017).

However, the sea level is a subtler information than the H_s, because offshore it is supposed to be very smooth, i.e. with very limited spatial gradients, while close to coast there is often great variation in the signal over short spatial and temporal scales. This is because of a number of physical processes that, especially in stormy conditions, lead to strong spatial gradients. On the other hand, these are the conditions we are most interested in, and when we badly need data.

It is obviously difficult to come across the lucky chance of a successful altimeter pass at the time and position of a severe event. Therefore, we follow a two-steps approach. For the benefit of the remote sensing side of the two interacting communities, in Section 2 we describe, albeit in very compact terms, the main oceanographic processes leading to substantial η differences and gradients in coastal areas. This part is substantiated with a rare, but exhaustive, example due to the unique availability at one specific location of both offshore and coastal data during a severe event. In Section 3 we explore a Sentinel-3A pass in the northern Adriatic Sea, East of Italy, to discuss the coastal problems and an anomalous altimeter signal. In Section 4 we move to the Sentinel-6A altimeter. Anticipating its regular flow of information, we explore two passes of one of the Jason.s satellites along its same orbit to describe two wind and wave events in the Adriatic Sea and how the Jason altimeter information compares with the corresponding model values. Granted the superposition and useful intercomparison between altimeter and model data, the results strongly suggest that both sides have to gain from each other, each source providing information not available, presently at least, from the other one. This stresses the need for an optimized and constructive use of both models and altimeters as sources of information that we highlight in the final summary.

Along the paper, we cite repetitively wave and surge model results. To appreciate fully the quality of these data we provide in Appendix A a compact description of the related meteorological, surge and wave models characteristics.

Appendix B provides the information where to find the data used throughout the paper.

2. The processes at work

In this section we provide a compact but adequate description of the main oceanographic processes at work in coastal waters.

Although our instinctive view of the ocean is two-dimensional, depth is instrumental in determining the physics of the ocean. It is certainly true that the major exchanges (energy, momentum, mass, spray, heat, etc.) with the atmosphere take place at the surface. However, the inner consequences, albeit with different time scales, are felt on the whole water column. It is intuitive that, the more limited the depth, the more affected the whole column is at once. Indeed, for more than one process the effect we see at the surface is strictly connected to the local depth. Therefore, at least for some processes, the shallower depths we find approaching the coast imply more manifest, i.e. enhanced, local consequences. The related details may depend on the input conditions from the atmosphere and the offshore conditions, on the geometry of the coast and, most of all, on how the local depth varies approaching the coast.

The key point is that for several processes the surface effects, the one we mostly care about, depend on the inverse of the local depth. It follows that often we find very large effects when approaching the coast. Of course this is the reason of the enhanced attention, of both the oceanographic and satellite communities, on this area. Several processes concur, at the first order of relevance, to these effects.

2.1. The processes and their physics

The physics of astronomical tidal prediction, in both the open ocean and coastal areas, is well known, see, among others, Pugh (1996). Although often amplified in coastal waters, a tidal wave does not imply the local strong spatial gradients requiring the 300 m resolution of the SAR mode of Sentinel-3A for their identification. These gradients are on a much larger scale, and they will not be dealt with here.

a- Wind stress and storm surge distribution – In a highly simplified description, the wind acting on the sea surface pushes the water in the wind direction. The key factor is the so called wind stress $\tau = C_D \cdot U_{10}^2$ (see, among others, Shi and Bourassa, 2019), with C_D the drag coefficient at the surface, and U_{10} the local ten metre wind speed. τ is instrumental in determining the local input of energy and momentum into the ocean, partly as current, partly as wind waves. Granted that a real situation is always a transient condition, once enough water has been piled up against the coast, the wind stress is counteracted by the surface steepness η'. The dynamical equilibrium implies $\tau = \eta' \cdot d$, with d the local depth. It follows that, approaching the coast, with decreasing depth d, η' must become larger and larger. Therefore, the highest levels of surge are found at the very coast, with substantial spatial gradients close to it.

b- Wave set-up – Moving to shallower and shallower water while approaching the coast, waves break and "throw" water towards the coast where it piles up increasing the local sea level. The process has been fully described and formalised in a series of papers by Longuet-Higgins and Stewart (the most complete one dates 1964). The basic physics is that waves transport momentum that increases with the significant wave height H_s. While waves approach the coast in progressively shallower and shallower water, after an initial growth due to shoaling, depth induced breaking (see Battjes and Janssen, 1978) steps in, progressively reducing H_s while approaching the shore. It follows that the momentum flux negative gradient (because of reducing H_s) must be counteracted by a positive one of the local sea level. The ensuing sea level spatial gradient depends dramatically on the bottom profile. If the bottom slopes-up progressively, the loss of momentum is distributed along the wave path. On the contrary, if the bottom slopes-up abruptly at the coast, most of the wave momentum is lost in a single go in very shallow water, then highly increasing the resulting so-called wave set-up and local sea level spatial gradients. An order of magnitude of the coastal wave set-up is given by the

coastal engineers' thumb-rule (derived from previous experience) that the related coastal sea level rise is 1/6 of the offshore significant wave height. However, as just specified, the actual figure is strictly related to how the depth decreases approaching the coast.

c- Combining surge and astronomical tide – The sea level at a given location is of course the sum of the contribution of the processes we have briefly described. Summarizing into "surge" all the wind and wave effects on the sea level at the coast, the overall resulting sea level depends on the relative time with respect to the astronomical contributions. As just hinted to at the beginning of this section, the theory and practice of tides are well known, tides are well forecast, both in time and as quantification. Although, especially in relatively shallow water, there is some reciprocal influence, the surge and astronomical contributions are to a large extent independent. However, what becomes crucial is time because the overall local sea level depends dramatically on the relative timing of the two peaks. We will provide a practical example in the following sections. Indeed, this is where reliable and timing information is badly required.

It is evident that, to have a full picture of the situation, we need information on both time and space. However, apart from satellites, in almost all cases the locally measured information is available at just one point, typically at the coast via a local tide gauge. It is therefore difficult to provide practical examples of actually measured spatial gradients that in most cases we see reflected as time variations in the single point records. However, in Venice we have this possibility. Together with a very intense practical case, this is what we describe in the next sub-section.

2.2. The CNR-ISMAR tower and the storm of 29 October 2018

The Adriatic Sea (Fig. 1, left panel) is the elongated basin to the East of Italy. About 700 km long, 200 km wide, bordered on both sides by relevant mountains, it is characterized by two main wind regimes. Bora, a frequently cold, strong and gusty wind, blows across the basin from North-East. Sirocco, a warmer, more stable wind, blows from South-East all along the basin. Though on average less strong than bora, it is however responsible for the most severe wave storms in the northern part of the basin. In particular, it is responsible for the floods that frequently affect Venice.

Approaching the coast, bathymetry has different characteristics on the west and east sides of the basin. On the former, as also on the northern end, the bottom slopes up gradually towards the coast, leading to enhanced local shallow water effects. On the contrary, the east side is characterized by deep water till the rocky coast. A general view of the Adriatic bathymetry is given in the later Fig. 7. Moving offshore, the map shows the 10, 20, 40-m isobaths. These are the ones of interest to judge the processes close to coast.

On 29 October 2018, a strong and extended storm (henceforth "the Storm") affected the northern part of Italy, both on its western (Ligurian Sea) and eastern (Adriatic Sea and eastern Alps) sides. Cavaleri et al. (2019b) provide a full description of the related events and modelling. For our present purposes we focus our attention on the most northerly part of the Adriatic Sea (Fig. 1b). The oceanographic tower Acqua Alta (see Fig. 1c, and panel b for its position) is located 15 km offshore, on 16 m depth (Cavaleri, 2000). Fully instrumented for meteorological (in particular, wind) and oceanographic measurements (waves, currents and tide), together with the tidal data available at the coast, it provides a full picture of how the local situation evolves in time and space. For our present purposes we describe the spatial distribution of the sea level in this coastal area, and how it evolved during the Storm in relation to the cited processes of (see the previous sub-section) a) storm surge distribution, b) wave set-up, c) combining surge and astronomical tides. Besides, we will report a unique example of how wind can suddenly affect the local sea level distribution. As already specified, our purpose is to offer a fully documented example of the possible sea level time and spatial gradients in coastal areas.

Fig. 2 shows the distribution of the surge elevation in the northern part of the Adriatic Sea at 18 UTC of 29 October, as simulated by the hydrodynamic model SHYFEM (see Appendix A).

In relation to point 2.1.a, it is evident that the most dramatic sea levels happen mainly at the north-west end of the basin. Note also that this is only the meteorological surge.

Fig. 3 provides the time history (36 h, from 29 October 00 UTC to 30 October 12 UTC) of respectively the significant wave height at the tower
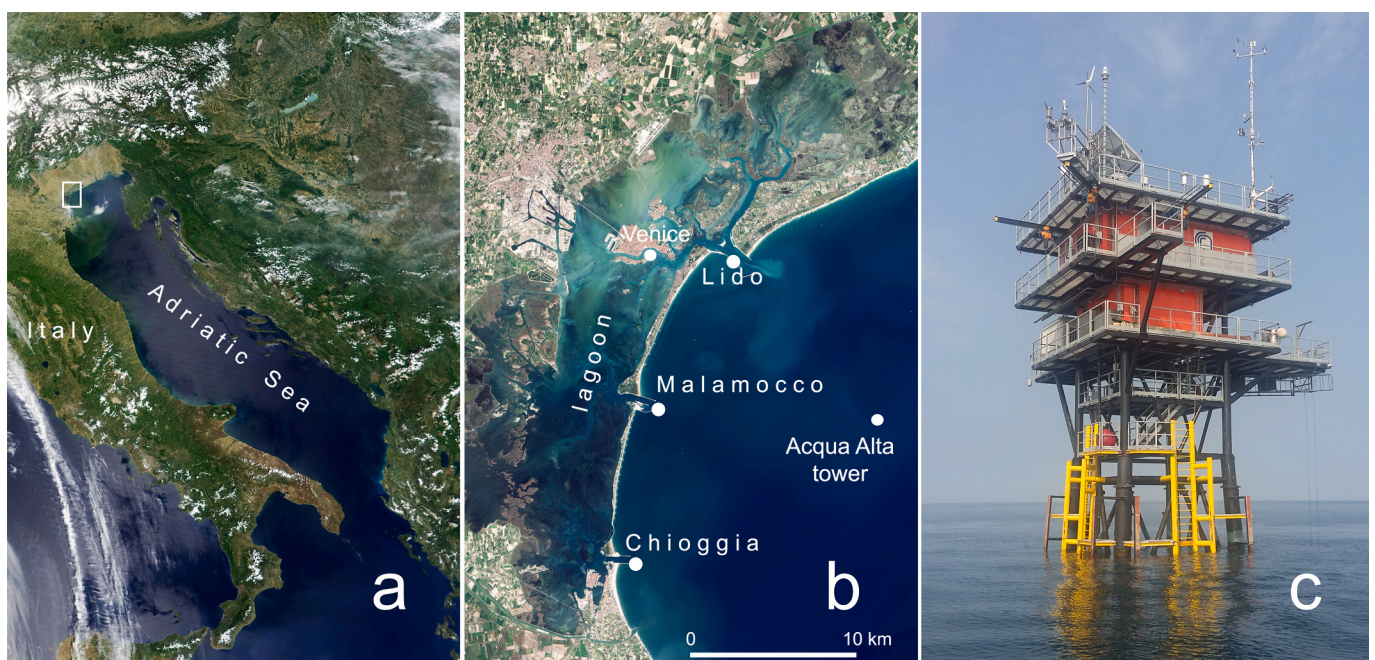

Fig. 1. a) Italy and the Adriatic Sea. The small rectangle shows the area in front of the Venice lagoon enlarged in panel b. b) Venice lagoon and the three inlets connecting it with the northern Adriatic Sea. c) Acqua Alta oceanographic tower. See its position in panel b). The dots show the position of the tide gauges cited in the main text.
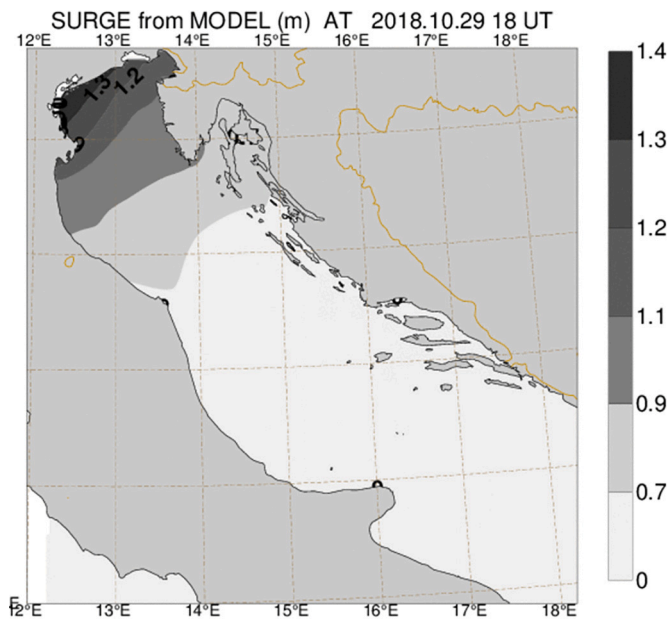
Fig. 2. Distribution of the surge elevation (m) in the northern part of the Adriatic Sea. See Fig. 1 for a general and detailed view of the area. Time is 18 UTC of 29 October 2018.
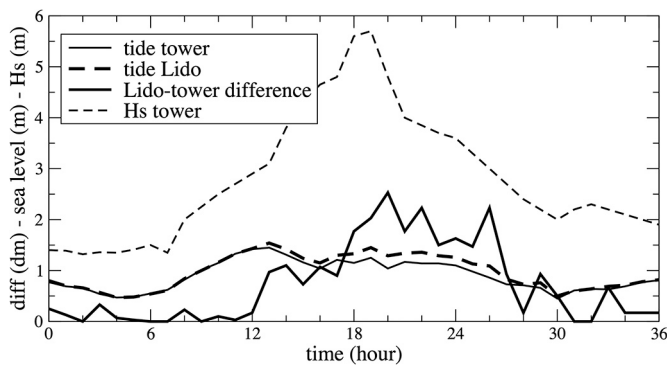

Fig. 3. Relationship between the significant wave height H_s at the tower (see Fig. 1) and the sea level difference between Lido and the tower tide gauges. Time is 29–30 October 2018.

(maximum H_s close to 6 m), the tidal data at the tower and the coast (Fig. 1b), and the related tidal differences. This is an example of the wave set-up described at point 2.1.b. Note in particular how the sea level difference between the Lido tide gauge and the tower closely follows the evolution of the significant wave height H_s. For a proper quantification of the implied gradients, we point out that the Lido gauge (Fig. 1b), at the end of the jetty, is located 2 km offshore, on about 6 m depth.

Indeed, as reported by several visual observations, the wave set-up increase of the local sea level was much higher at the beach.

Although hit by the 29 October flooding, most Venetians ignore how lucky they have been. Fig. 4 shows the evolution of the astronomical tide, the surge and the resulting sea level (i.e. the one actually measured). The period is again from 29 October 00 UTC to 30 October 12 UTC. While the local maximum happened around 12 pm of October 29, please note how the peak of the surge was at 18 UTC. This was during the trough of the astronomical component. Had the wind hit six hours in advance, the maximum level would have been more than half a metre higher. In connection also to Fig. 2, it is easy to guess how large the spatial gradients may have been. On a side note we point out that Venetians were not so lucky one year later, on 12 November 2019, when a more limited surge, but in phase with the peak of the spring tide, added
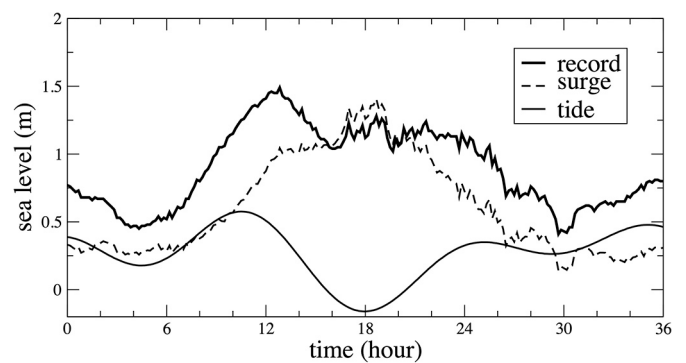

Fig. 4. Sea level evolution in Venice on 29–30 October 2018. Note how the peak of the surge happened at the minimum of the astronomical tide. See the text for the discussion of the implications.

to also other factors, led to what for only a few centimetres was not the worst flood in history. The interested reader can find a full description in The ISMAR Team (2020).

Going back to the Storm, we conclude our examples from October 29 showing in Fig. 5 the detailed (data at 5 min interval) sea level history at the tower, Lido and Chioggia (see Fig. 1b for their position). The figure covers the 3.5 h period 17.00–20.30 UTC (hh.mm, from 0 to 210 measurement ticks). Note the sudden (in about 10 min) 20 cm drop of the sea level at the tower at tick 105. On a different scale (both horizontal and vertical) and less impressive because of the hourly data interval, the change is visible at 19 UTC also in Fig. 3. The reason, fully explained in Cavaleri et al. (2019b), is a sudden change of the local incoming wind direction from South-East to South-West. This implied that, instead of blowing towards the coast, the wind became parallel to it. This (see again sub-section 2.1.a) led to the sudden disappearance of the wind stress towards the coast, and the consequent partial collapse of the local surge. Note how, on a different scale, something similar happened half an hour earlier at Chioggia (Fig. 1b). The time difference corresponds to the time required by the meteorological front to move (at about 40 kmh^{-1} translation speed) from Chioggia to Lido (20 km away). What described above provides a quantitative idea of the spatial gradients that may appear in coastal waters. Although locally remarkable, this example is by no means unique. As an extreme example, think that Katrina, the 2005 destructive hurricane in the Gulf of Mexico, led to an 8 m surge to the East of New Orleans (see, among others, Cavaleri et al., 2018).

We have described the Venice episode in detail simply because of the unique opportunity of both coastal and offshore, although still close to the coast, measured data and the consequent documented quantification of the gradients involved. To complete the picture we discuss the potential use of the Sentinel-3 SAR mode and standard altimetry data in

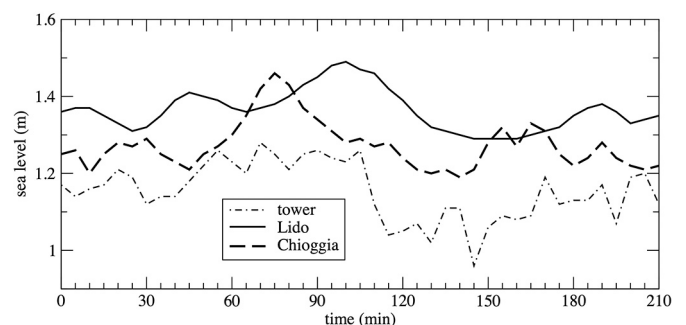### sea level history at tower, Lido and Chioggia

Fig. 5. Sea level variations at the tower and two coastal gauges. See Fig. 1 for their position. Note the drastic changes (at 105 min at the tower on the figure) at the passage of the cold front. See text for the full explanation.

inner and coastal seas. We analyse a number of passes in the Adriatic Sea, exploring the accuracy of the signal, both on itself and versus the results of an amply verified local sea level model. This is the subject of the next two sections.

3. A Sentinel-3A pass on the northern Adriatic Sea

In a previous paper (Cavaleri et al., 2019a) some of us had analysed a Sentinel-3A pass in very coastal waters. The track is shown in Fig. 6a (used in the cited reference). The descending pass was at 09.44 UTC 25
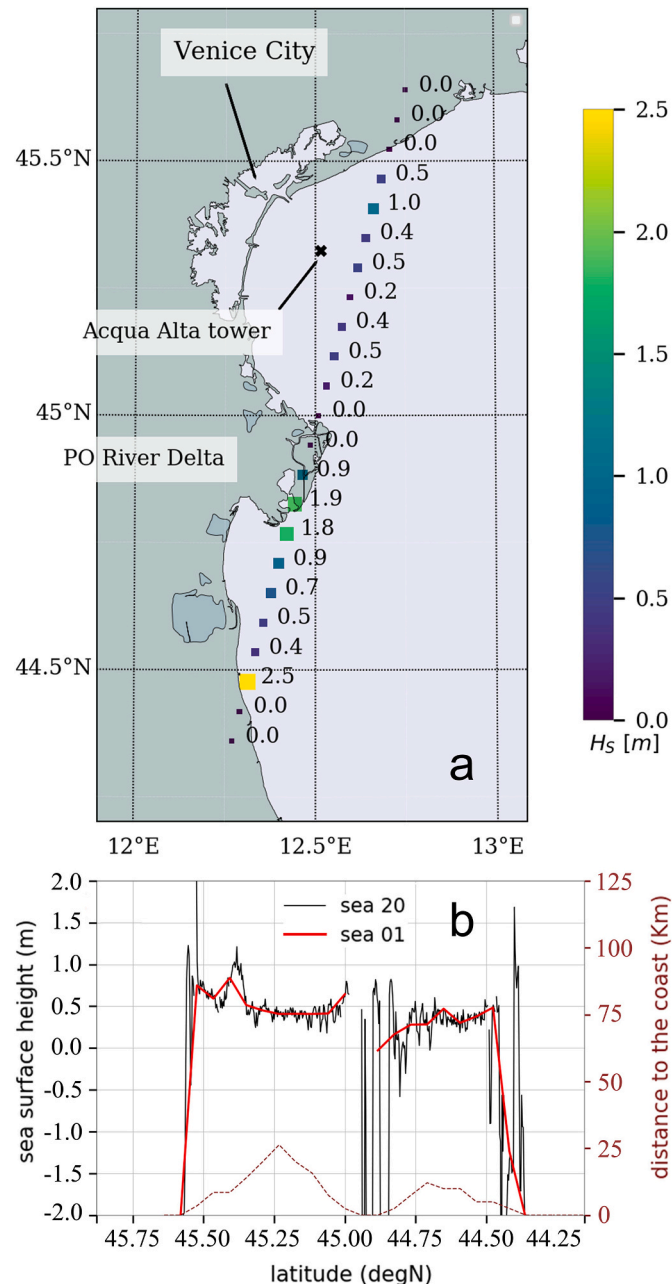
July 2017, entering the sea East of the Venice lagoon, at about 45.50° N, passing offshore Venice, barely touching the Po river delta, and then, after another short distance on water, ending on the Italian peninsula at 44.50° N, covering just slightly more than 100 km. Cavaleri et al. (2019a) used a Level 2 product provided from the Copernicus service with identifier: "S3A_SR_2_WAT_20170725T094431_20170725T0 94658_20170725T120008_0146_020_193_MAR_O_NR_002.SEN". In the figure the 1 Hz measured significant wave height H_s values are reported near the corresponding measurement positions. Apart from expected anomalous values close to coast (see the Po river delta and the final landing point), attention had been called to the isolated 1.0 m H_s value shortly after exiting into the sea. Note that measured and modelled wave height values were of the order of 0.4 m. At the time attention was called to this singular high value, without any explanation.

Focusing on the sea level data, we have explored the same pass to see if there was any correlation between the two different measured data. The main result, although in a different format, is given in panel 6b. The pass, with decreasing latitude, goes from left to right. We show the 20 Hz estimations and the 1 Hz data, both from the SAR mode. The dashed line indicates the distance (km, right scale) from the closest land. Apart from the noise on the Po delta and at the final landing point, the feature we focus on is the bump, evident in the 1 Hz data, but more macroscopic in the 20 Hz signal, around 45.32° N. This is exactly the position of the previously cited H_s bump. Of course this can hardly be a chance, and we looked for an explanation. Note that the corresponding model distribution (not shown to avoid another overlapping line) is pretty smooth, as it was in the case of wave height. A first possible culprit could have been the oceanographic tower seen in Fig. 1c (position in 1b and panel 6a). The tower has a 5×7 m^2, 15 m tall, extension, but it was 12–14 km off the ground track. It was actually closer 2 s later (see panel 6a). Ships, sometime abundant in the area, are regularly moored to the West of the tower, so off the track. Following the interesting paper by Tournadre (2014), which describes how to analyse the shape of the altimeter return signal to detect icebergs or ships, we asked him to look at the above pass to detect any possible reason for the bump. Rain effects were excluded, both from local meteorological reports and the absence of cloud liquid water in the remote sensing signal (the rad_liquid_01 parameter). However, there is clearly a strong attenuation at nadir in both KU LRM, C and Ku SAR that strongly distorts the waveform and leads to erroneous geophysical parameters. The backscatter is also very high, and there is a sigma bloom with small scale variability of sigma0 which makes the Brown model invalid. The most likely explanation, suggested by another colleague (see Acknowledgements) and confirmed by Jean Tournadre, is the crossing of the altimeter ground track with a "river_into_the_sea", a surface flow of fresh water exiting from the very close Sile river exit.

4. Jason.s profiles on the Adriatic Sea

Planning to work with the altimeter data of the Sentinel-6 altimeter, we resorted to the Jason passes, which follow the same repeated passes tracked also by Sentinel-6, looking for suitable episodes of the recent past. We used the latest along-track regional data provided by the Sea Level Climate Change Initiative (Climate Change Coastal Sea Level Team, 2020) (SL_cci), which are retracked using the ALES subwaveform retracker (Passaro et al., 2014) and corrected using the X-TRACK Processor (Birol et al., 2017). We chose this dataset because it has been demonstrated to significantly improve the performances of the altimeter in the coastal zone while maintaining the quality in the open ocean and because it is provided 20 Hz measurements with a dedicated analysis of their average performance (Birol et al., 2021). We focused on relatively recent events (a few years ago at most) to be sure to have corresponding reliable and accurate model data.

CNR-ISMAR (henceforth ISMAR) has a daily activity of analysis and forecast on the whole Mediterranean Sea, with a special attention on the Adriatic Sea. There is an obvious direct interest on Venice and its surrounding area (see Fig. 1), but the main physical reason is that the

Fig. 6. a) Detailed geometry, focused on the area of Fig. 1b, of the northern part of the Adriatic Sea in front of the Venice lagoon. Dots and numbers show the single significant wave heights at 7 km interval from the pass of Sentinel-3A altimeter at 09.44 UTC 25 July 2017 (after Cavaleri et al., 2019a). b) Sea level distribution along the same pass. Both 1 Hz averages and 20 Hz estimations from the SAR model of the Sentinel-3A mission are shown. The dashed line indicates the distance (km, right scale) from the closest land. See the main text for the specific information on the pass.

geometry and meteorology of the area lead to intense phenomena, like localized surge elevation, and strong coastal sea level gradients in the most northerly part of the basin.

Fig. 7 shows the useful passes on the Adriatic Sea with their respective numbers and flight directions. Exploring the previous pass times and corresponding meteo-oceanographic conditions, we focused our attention on two episodes, pass 161 on 26 November 2015 and 196 on 16 November 2014. The two episodes represent the two typical situations of the Adriatic basin, with respectively bora and sirocco conditions. They are now separately analysed.

4.1. 26 November 2015–161 pass at 11.30 UTC

The wind and wave situations (at 12 UTC) are shown in Fig. 8, respectively on panels a, b. There is a sustained North-East coming wind, blowing towards the Italian coast, particularly in the area of the pass, indicated in panel a. More on this in the discussion in the next section.

The situation suggests the presence of piling-up of water against the Italian coast (due to wind stress), with a further increase very close to the coast where, due to the shallow water (see Fig. 7), waves break leading to the (see Section 2) wave set-up. Wind speed along the pass was about 15 ms^{-1}, H_s slightly less than 2 m.

It is instructive to analyse the altimeter data, first separately, and then compared to model. These are shown in Fig. 9 which requires a bit of explanation, especially for oceanographers.

Aiming at exploring the ideally undisturbed sea level, the altimeter-detected values are corrected for tide and Dynamic Atmosphere Correction (including inverse barometer effect and wind stress effects), as well as other instrumental and atmospheric corrections, to obtain the Sea Level Anomaly. The sum of sea level anomaly, ocean tide correction and dynamic atmosphere correction is from now on identified as "Sea Level" in the figures of this paper concerning altimetry data. See Andersen and Scharroo (2011) for a related full description of the procedure. The derived "corrected" 20 Hz data are the very noisy almost horizontal signal (left to right, from Italy to Croatia). Instead of simply averaging the 20 Hz retrievals to obtain a 1 Hz value, we smooth the 20 Hz signal using a running mean with a 1 Hz window. The procedure is particularly effective close to coast, the 20 Hz smoothed data allowing observation up to 3–4 km from the coastline. We will soon be back on

Fig. 7. Ground tracks of the Jason.s and Sentinel-6A altimeter passes on the Adriatic Sea, East of Italy. The following figures focus on, respectively ascending and descending, passes 161 and 196. Note the general bathymetry of the basin, focusing mainly on the 10, 20, 40-m isobaths along the coastline.

this point.

As oceanographers, our practical interest is on the actual sea level, the one relevant for, e.g., the flooding of Venice. So, knowing the corrections, we went back to the original signal adding back tide and Dynamic Atmosphere Correction. More immediate in the filtered signal, there is a clear up-slope moving in the wind direction, from Croatia (right) to Italy (left in the figure).

Before comparing altimeter and model data, a comment is due on the altimeter initial and final pass values in this flight section, close to the two coasts. The noise on the Croatian coast is expected because of the presence of large and small islands (we will have a nice example for pass 196). However, there is a progressive decrease of the filtered signal on the Italian coast. Given the meteo-oceanographic situation seen in Fig. 8 and the physics described in Section 2, notwithstanding the lack of on-the-spot measured data, it is unlikely this corresponds to a physical truth. Focusing on the altimeter data and looking at the corresponding unfiltered signal in Fig. 9, the decrease appears to be caused by a series of 20 Hz retrievals very close to the Italian coast, which estimate a lower sea level than the points located further away.

Another possibility is that, when moving from land to coast, the on-board tracker of the satellite hooks a leading edge of the returned signal that does not correspond to the coastal waters located at nadir (for an explanation of the hooking effect in altimetry, which is also typical of inland waters, see for example Boergens et al., 2016). Besides, wrong estimations of significant wave height (for example due to the hooking) may lead to a wrong sea state bias correction (computed at 20 Hz rate in the dataset we use, see Marti et al., 2019), which is then applied to the range estimated by the satellite in order to derive the sea level.

Granted the likely problems of the altimeter signal at the two extremes, it is now instructive to compare it with the corresponding model profile along the same track. The model is the operational one at ISMAR (Ferrarin et al., 2013). The results are given in Fig. 10 where for Jason we use only the non-corrected and filtered signal. Note that, because of the difficulty of a common reference level, what is important in the comparison are the trends, not the absolute values. Given its high resolution, the model is able to represent the sea level also in the inner space among the islands (the large one is Cres) and the Croatian coast, where the altimeter has no room for manoeuvre. Note also that there is half an hour difference between the pass and the model times.

In general, there is a nice fit between the two profiles. Excluding the two coastal extremes, the mean "model-altimeter" difference is 1.25 cm, the r.m.s. difference is 2.7 cm. Some minor discontinuity of the model data is due to the selection of the closest knot in the unstructured grid of the model. An interesting feature is a clear faster growth of the altimeter derived sea level when we move offshore, hence westwards, from the last Croatian coast (Cres island), from 14.0°E till 14.3°E. In our interpretation, based on long term local experience, the likely reason is the underestimate, by the meteorological model, of the offshore blowing wind speed. Cavaleri and Bertotti (2003, 2004) have repetitively stressed the underestimation of the ECMWF (European Centre for Medium-Range Weather Forecasts, Reading, U.K.) wind speeds in the Adriatic Sea. This is more the case for bora, as in the present episode. This has been attributed to a not sufficiently detailed orographic description and, typical of most models, a slow catch-up of the wind speed when entering sea from land.

The MOLOCH meteorological model (see Davolio et al., 2017, and http://www.isac.cnr.it/dinamica/projects/forecasts) used to drive this surge simulation has a much higher (1.4 km) resolution. One possibility, suggested by the evidence in Fig. 10, is that also at this resolution the model wind is slightly underestimated when blowing off the coast. Therefore we suspect that in this area the altimeter reveals the true profile that only later, in the middle of the Adriatic Sea where the wind achieves its full accuracy, fits well with the model results.

Another feature that we discuss extensively in the next section is the smoothness of the model profile compared to the much more irregular output of the altimeter.
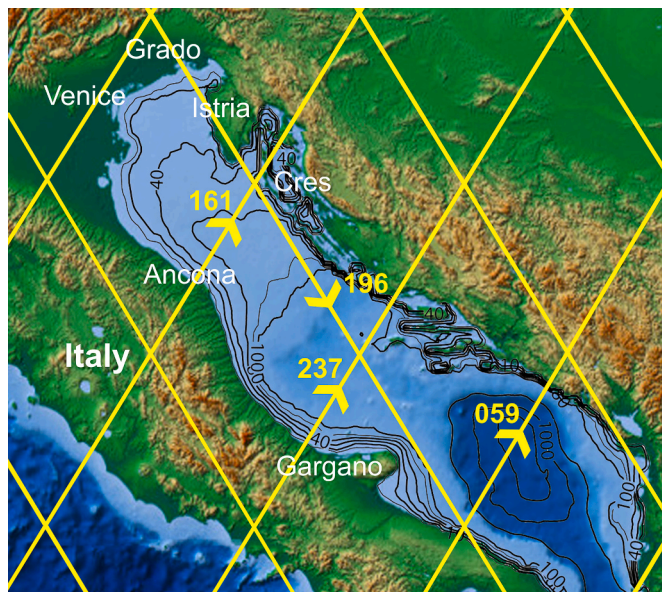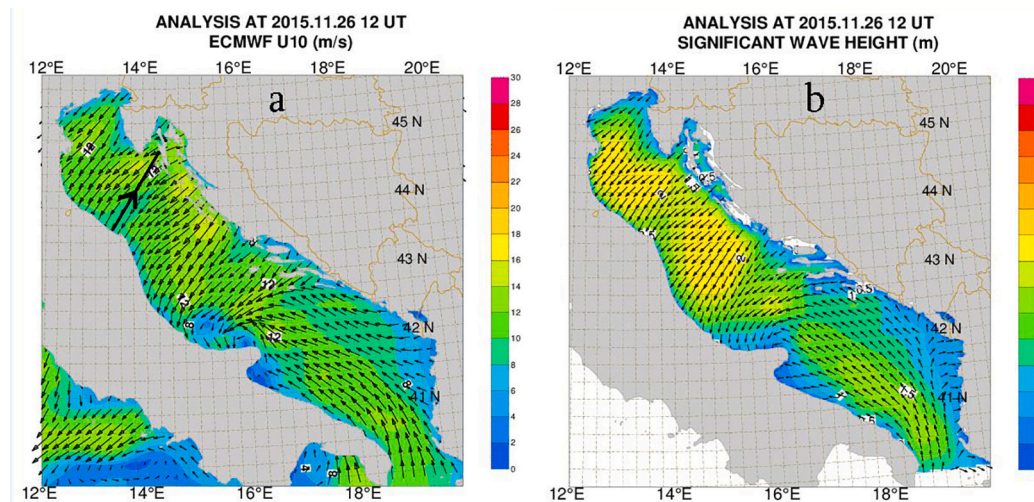
Fig. 8. a) Wind field in the Adriatic Sea (see Fig. 1 for the overall geometry) at 12 UTC 26 November 2015. The black line shows the ground track of pass 161 by the Jason altimeter. b) the corresponding significant wave height field.
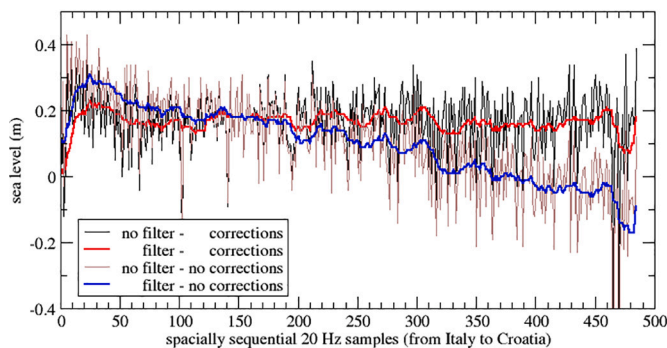

Fig. 9. With reference to the pass in Fig. 8, 20 Hz and filtered sea level profiles. Both the corrected (for tide and wind stress) and original data are shown. Note the obvious up-slope towards the Italian peninsula (left side of the plot).
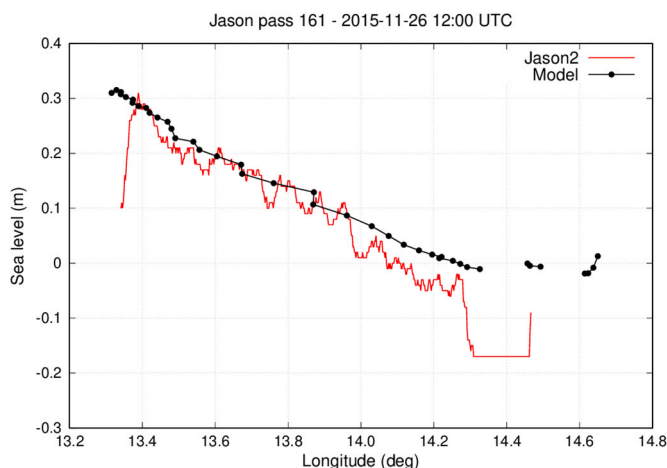

Fig. 10. With reference to the pass in Fig. 8, comparison between the original, but filtered, altimeter sea level in Fig. 8 versus the corresponding model results.

4.2. 16 November 2014–196 pass at 01.30 UTC

Conditions were quite different, and purposely chosen, on 16 November 2014, with a sustained south-easterly wind on most of the Adriatic Sea, turning to North after the front that we see in Fig. 11a at about 14° East longitude. The wind is close to 14 ms^{-1} leading to the distributed North-West directed 2.0–2.5 m high waves in panel b. Note the turning to North of the field in the upper part of the basin, following the local northerly flowing wind.

The altimeter path is shown in panel a. Entering the Adriatic Sea at the edge of the Grado lagoon, at the basin upper end (see Fig. 7 for the specific location), there is a short sea track before entering Istria (the peninsula at the upper end of the basin, part of Croatia), then proceeding further along the whole basin. The path ends at the southern end of the Italian peninsula. Indeed, we were hoping to see here some local effects because of wind and waves blowing and moving practically perpendicularly to the local shallow coast. Note that shallow effects are missing on the Croatian side because of the rocky and quickly deepening coast.

In this 196 pass case in Fig. 12 we show directly the comparison between the model and altimeter sea level profiles along the track. Granted the irregularities of the (filtered) altimeter signal, there is a general good reciprocal fit, with an average "model-altimeter" difference of 0.18 cm, r.m.s. difference 4.3 cm. Both model and altimeter show the expected accumulation of water towards the northern part of the basin.

Several features are worth discussing. The altimeter signal shows extended very strong irregularities, notably at a scale longer than in the 161 pass. This may have an interesting geophysical significance that we discuss in the following section. The macroscopic features are the two ample oscillations of the altimeter signal at about 42° and 44.5° N. Note the much smoother and uniform trend of the model profile. A close inspection reveals that the 44.5° N "noise" is due to a tiny islet, to the West of the Cres island, located exactly on the Jason ground track. However, nothing similar is present at the other 'noisy' position, at 42° N. The only thing we note is that the noise appears at the track position closest to land (the Gargano peninsula), still 20 km away.

The model shows the expected coastal effects at the upper end of the track (but remember this is a descending pass). Here the combination of wind stress and wave set-up on the shallow coast of the Grado lagoon (see Fig. 11a) leads to relatively strong local gradients, that we recognize in the model profile as a steepening of the sea level when approaching the coast.

However, the section at sea appears too short for the altimeter to appreciate these details. Here, the interpretation of the altimetry profile
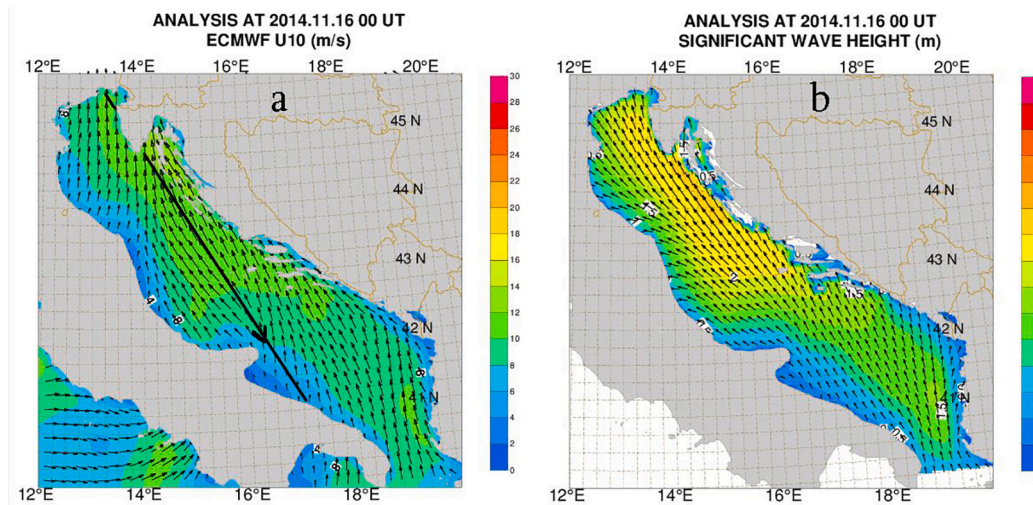
Fig. 11. a) Wind field in the Adriatic Sea (see Fig. 1 for the overall geometry) at 00 UTC 16 November 2014. The black line shows the ground track of pass 196 by the Jason altimeter. b) The corresponding significant wave height field.
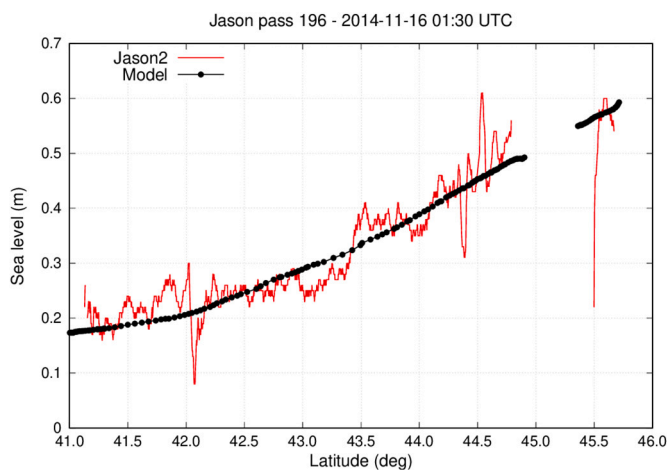

Fig. 12. With reference to the pass in Fig. 11, comparison between the original, but filtered, altimeter sea level profile versus the corresponding model results.

is particularly difficult. The SL_cci dataset contains an indication not to use 20 Hz data closer than 4 km from the coast. We have followed this indication before applying the running mean, nevertheless the strong sea level drop at 45.5 latitude may be the effect of residual outliers which are still present in the dataset close to the coast.

5. What we can learn and where to look forwards

It is clear that in these last few years much improvement has been achieved in extracting more and more information from the altimeter return signals, with a remarkable extension towards coastal waters. There is clear progress in the data handling of coastal altimetry sea level data in the latest SL_cci dataset. In line with the general trend, this study shows that coastal altimetry can now achieve accurate and useful results much closer to the coast than previously thought possible. However, this is only today limit.

For the present likely errors close to coast, we suggest they may be due to the hooking by the on-board tracker to the leading edge of the return signal not corresponding at nadir, i.e. at coastal water. In similar situations, this leads to a double error: the wrong interpretation of the direct signal, and also of the value of significant wave height and the consequent wrong sea state bias correction. At distances like the one

seen for track 161, the quality of the retrieval still needs improvement. This is where we have to work hard. Granted the large and long-term interests in the vast expanse of the oceans, both for large scale circulation and the very hot subject of sea level rising, the coastal environment represents what we can call the "everyday interest". The high density of population, the direct impact of currents and waves on the inhabited front-land, the stirring and transport of sediments and potential pollution, are all problems that, for a proper management and forecast, require detailed and frequent data.

Altimetry, although not as continuous as we would like it to be, provides an enormous volume of data throughout the globe. Although we still have problems when approaching the coast, both the Sentinel-3A SAR approach and the advances in the reprocessing of 20 Hz data from the LRM missions push, at least potentially, the useful results much closer to coast. In this coastal range a strong support is given by waves and sea level modelling.

Granted the approximations inherent to both the physics represented in the models and the driving meteorological input, models do imbed the most important physics, as, e.g., wind stress, tide, wave set-up. They can therefore provide a reliable reference truth for what is going on close to the coast and what the satellite instruments will, in due time, be able to see.

This is not the only synergic use of the two sources, i.e. satellites and models, and their data. Approaching the problem in what could be the wrong way, we had pointed out the very noisy profile of the surface sea level (see Figs. 10 and 12) provided by altimeters compared to the very smooth ones of the model. The same happens for significant wave height H_s, see, e.g., Cavaleri et al. (2019a) for the pass on the Po delta. However, the interesting, and fundamental, question is how much of this is noise and how much geophysical variability. For both physical approximations and numerical reasons, models tend to smooth the fields, both the wind ones and the sea surface geometry, as H_s and sea level. On the base of direct measurements on the sea, then suitably transferred to the operational models, Abdalla and Cavaleri (2002) have clearly shown the effect of wind gustiness and how this enhances the growth of wind waves. Mutatis mutandis, the same is true also for circulation and sea level because the driving wind stress is a non-linear function of the wind speed.

Wind speed gustiness depends both on orography (when close to coast) and air-sea stability conditions. See the nice series of examples reported by Komen et al. (1994), their Fig. 4.2). Working on the ISMAR oceanographic tower data (panel 1c), Abdalla and Cavaleri (op.cit.) related the dominant gustiness period of the bora wind both to the air-

sea temperature difference (hence stability conditions) and the steep orography of the coast the bora blows from. The basic period of the recurrent strong wind gusts was 20 min superimposed to the faster "random" variability (we stress that often "random" represents the limits of our knowledge). Bertotti and Cavaleri (2008) reported something similar in a very severe mistral storm in the Western Mediterranean Sea when a large cruise ship was heavily involved. At the time there was the lucky pass of the Jason altimeter all along the main axis of the storm. The H_s altimeter profile at 1 Hz interval showed a strong variability compared to the very consistent, but smooth, model profile. The authors wondered about the truth, oscillating between the hypothesis of a noisy signal, but also questioning the smoothness of the model profile. After all, talking about direct measurements of the oscillating sea surface, in pure statistical terms standard 20 min records in a storm lead to H_s values with 6% rms possible error. Indeed, looking with new eyes at the model and Jason profiles in Fig. 10, we wonder (see sub-section 4.1) if the oscillations of the sea level do represent, albeit with some approximation, a physical truth. A quick estimate indicates a spatial periodicity of about 6 km that with 15–16 ms^{-1} wind speed ($\sim$ 55 km hr^{-1}) corresponds to about 6–7 min periodicity, a realistic dominant gustiness period off the orography the wind blows from. But there is more. We have pointed out the more rapid sea level increase, with respect to the model, shown by the altimeter soon off the coast. We assign this to a slight underestimate of the offshore blowing wind speed, hence the lower model wind stress and the consequent slower pile-up of water towards the West.

The lesson we all have to learn is that we are dealing with two powerful tools, models and measurements, with a large superposition capable to offer cross-validation. Models, including a lot of physics, important especially (for the present purpose) in coastal waters, are well suited to represent the truth when the physics of the waves-sea level coupling implies large spatial gradients. We know these gradients are important for safety, management, but also for a better understanding of the local currents, sediment transport, and pollutant distribution. Here we badly need the measured truth, and altimetry is well on its way to dealing with these problems, although there is still a long way to go. However, from an opposite perspective our models appear somehow idealized in their distribution at large scale, a fact important for approaching the coastal problem with a correct and full information,. The hourly, often smoothed, driving input by wind hides the shorter scale variability of the atmosphere. The energy present in this relatively high frequency range of the atmospheric spectrum is not small and should be considered. At ECMWF this "hidden" input to waves is estimated on the base of the air-sea stability conditions and a theoretical estimate of the implied extra input (see the IFS documentation, part VII, at https://www.ecmwf.int/en/elibrary/19311-part-vii-ecmwfwave.model, section 3.2 for the details). However, our model outputs are always smooth, while the altimeter "truth" strongly suggests a more dynamical distribution of both wave heights and sea levels. We need to exploit both these sources of information. Our next challenge is to merge these two partially overlapping sources, each one improving on the base of the other one, to reach the full knowledge we need for an enlightened management of our environment, both at the coast and offshore.

6. Summary and conclusions

We summarize our main conclusions in the following main points.

1- There has been much improvement in the interpretation of the return altimeter signal concerning sea level. This is particularly true close to the coast where we find commonly the largest spatial gradients.
2- Two techniques have been, and are used in this respect: the SAR approach of Sentinel-3A and retracking of the 20 Hz altimeter return

signal from the LRM missions. Both these improvements in handling the radar signal would remain ineffective without reliable geophysical corrections to the raw range estimated by the altimeter.
3- Notwithstanding these improvements, much work remains to be done in order to get reliable detailed data closer to coast, particularly along the last 3–4 km, which is the average distance at which on average the correlation of SL_cci data against tide gauges starts to drop.
4- For this purpose a fundamental support is provided by high resolution wave and sea level numerical models. The detailed and sound description of the implied physics, in particular close to the coast, offers the necessary know-how for further improvement of the information to be derived from the altimeter signals.
5- More in general, altimeters and models must be considered as complementary information. Neither is complete, but both provide superimposed, hence comparable, information, covering ground partly out of the other range.
6- In one of the cases we dealt with, the altimeter-derived coastal sea level profile has suggested a model limitation that we associate to a not sufficiently strong wind speed when blowing off the coast.
7- More in general and still an open problem, the general altimeters sea level profiles reveal a much more articulated surface distribution compared to what is usually suggested by models. Not part of this paper, the same is true for the significant wave height information.
8- For models, granted their intrinsic approximations, this is also connected to the smoothed input meteorological information and to a partial lack of knowledge in the high frequency tail of the respective data and physics.
9- Granted a necessary step also in theoretical knowledge, the synergetic use of altimeter and model data is a primary guide line for further improvement in this direction.

Author statement

L. Cavaleri: conceptualization, formal analysis, investigation, writing original draft. **L. Bertotti**: data curation, software, validation. **C. Ferrarin**: Software, data curation. **M. Passaro**: data curation, funding acquisition, validation, visualization. **P. Pezzutto**: data curation; A. Pomaro supervision, visualization. All authors have contributed to review and editing

Declaration of Competing Interest

The authors declare that they have no known competing financial interests or personal relationships that could have appeared to influence the work reported in this paper.

Appendix A. Hydrodynamic, meteorological and wave models

We provide here a compact description of the meteorological, circulation and surge, and wave models used to derive the estimated elevation and wave fields to be compare with satellite data. Apart from the barely touched technicalities of the model structure, we focus on the accuracy of the results to appreciate fully the discussion when comparing satellite data with our estimate of the corresponding sea truth.

A.1. Hydrodynamic and meteorological models

The 3D hydrodynamic model SHYFEM (Umgiesser et al., 2014) was applied to simulate the sea levels in the Mediterranean Sea. The horizontal discretization of the state variables is carried out with the finite element method, with the subdivision of the numerical domain in triangles varying in form and size. Vertically the model applies Z layers with varying thickness. The boundary conditions for stress terms (wind stress and bottom drag) follow the classic quadratic parameterization. The Smagorinsky's formulation (Smagorinsky, 1963) is used to parameterize the horizontal eddy viscosity. For the computation of the vertical viscosities, the solution is provided by a turbulence closure scheme. This scheme is adapted from the k-ε module of GOTM (General Ocean Turbulence Model) described by Burchard and Petersen (1999). A detailed description of the model and its validation over the Mediterranean Sea is given by Ferrarin et al. (2013, 2018) and Cavaleri et al. (2019b).

In this study, the altimeter data are compared with the results of the operation implementation of the SHYFEM model over the Mediterranean Sea. On average, the total water level simulated for the first forecast day had correlation 0.86 and a root-mean-square error of 5.4 cm with measured data (Ferrarin et al., 2013). The forecasting system consists of the finite-element SHYFEM model, that includes an astronomical tidal model, coupled with a finite element spectral wind wave model. The modelling system account for non-linear interaction of tide and surge in shallow water (Horsburgh and Wilson, 2007; Williams et al., 2016) and for the effect of waves on the coastal sea level (Longuet-Higgins and Stewart, 1964).). The unstructured numerical grid model covers the whole Mediterranean with approximately 140,000 triangular elements and a resolution that varies from 10 km in the open sea to 3 km in coastal waters and less than 1 km on the coasts of Italy. SHYFEM is forced at the water surface by 10 m wind and mean sea level pressure generated by a numerical weather prediction chain implemented operationally at the Institute of Atmospheric Science of the National Reseach Council (CNR-ISAC, http://www.isac.cnr.it/dinamica/projects/forecasts). Such model framework comprises the hydrostatic model BOLAM (which covers Europe and the whole Mediterranean Sea) and the non-hydrostatic model MOLOCH (which covers Italy and the whole Adriatic Sea), nested in BOLAM. The MOLOCH model is implemented with a horizontal grid spacing of 1.4 km. This model chain has already been successfully validated over the Adriatic Sea (Davolio et al., 2015; Stocchi and Davolio, 2017).

A.2. Wave model

The wave conditions in a basin are estimated using a spectral wave model. A thorough description of the related technicalities is given by Komen et al. (1994). An easier approach is found in Holthuijsen (2007). The sea conditions at each location are considered as the superposition of a number of sinusoidal waves, specified as amplitude (hence energy), frequency and direction. Typically 30–35 frequencies are considered (e.g., from 0.03 Hz up to 1.0 Hz) and 24 or 36 equally distributed directions. The evolution in space and time of each component is estimated quantifying all the processes that concur to add, dissipate or exchange its energy. The basic input information are the driving wind fields and the geometry of the basin, including depth. Considering the significant wave height, mean and peak periods, and direction of the wave fields the present quality of the wave model results is extremely good. Compared to satellite and buoy measured data the wave height differences are of the order of 1% or less, see the performance of the European Centre for Medium-Range Weather Forecasts (ECMWF, Reading, U.K.) by Bidlot (2019). Using this Centre meteorological data as input information, the wave conditions in the Adriatic Sea (see Fig. 1) are estimated using the WAM wave model (Komen et al., 1994) on a $(1/12)^o$ resolution grid. Repeated comparisons with the data collected at the CNR-ISMAR oceanographic tower (panel 1c, see Cavaleri, 2000) suggest an accuracy of the local wave heights of the order of a few percent (Cavaleri et al., 2018).

Appendix B. Data used throughout the paper

B.1. Altimeter data

In Section 4 we use the regional XTRACK/ALES altimeter along-track multi-mission high frequency sea level anomalies, v1.0, available from http://www.esa-sealevel-cci.org/products. The product contains along-track regional sea level dataset specifically processed to enhanced the performances in the coastal zone. It has been recently validated against tide gauges (Birol et al., 2021), showing a large increase in the percentage of available coastal sea level data from Jason-1 (valid data up to 3.6/1.9/0.9 km from the coast on average with Jason-1/Jason-2/Jason-3). The list of the parameters and geophysical corrections is reported in Table 1 from Birol et al. (2021).

Table 1
List of altimetry parameters and geophysical corrections used in the computation of X-TRACK/ALES coastal sea level product.

Parameter	Source	Jason-1/Jason-2/Jason-3
Altitude	GDR	Altitude of satellite
Range	ALES/TUM	20 Hz ku band ALES corrected altimeter range (Passaro et al., 2014)
Ionosphere	GDR	From dual-frequency altimeter range measurement
Dry troposphere	GDR	From ECMWF model
Wet troposphere	University of Porto	GPD + radiometer correction (Fernandes et al., 2015)
Sea state bias	ALES/TUM	Sea state bias correction in ku band, ALES retracking (Passaro et al., 2018)
Solid tides	RADS	From tide potential model (Cartwright and Taylor, 1971, Cartwright and Eden, 1973)
Pole tides	GDR	From Wahr (1985)
Loading effect	RADS	From FES 2014 (Carrere et al., 2012)
Atmospheric correction	RADS	From MOG2D-G (Carrere and Lyard, 2003) + inverse barometer
Ocean tide	RADS	From FES 2014 (Carrere et al., 2016)

The datasets adopt specific solutions in terms of range and sea state bias, which improve the quality and the quantity of sea level retrievals compared to standard open ocean processing. Moreover, it is important to consider the choices of corrections for the atmospheric delays, which require particolar attention in the coastal zone. Delays caused by the interaction with the atmosphere can be corrected by comparing range measurements at different frequencies (for the delay due to the ionosphere) or by using radiometer measurements (for the delays due to the troposphere). In both cases, these techniques are affected by the presence of land (Fernandes et al., 2014). The delays can also be derived using modelled data, which nevertheless may have suboptimal space and time resolution. This is particularly the case for the delay caused by the water vapour (called the wet troposphere correction), for which a combined solution using radiometer measurements, in-situ measurements from coastal stations and model data (Lazaro et al., 2020) have been adopted in the framework of SL_cci.

B.2. Data availability

We provide here the information on how to access the files used for the new analyses carried out in this paper. For the example in Section 3, the reader is referred to the original paper by Cavaleri et al. (2019a).

For each one of the two passes 161 and 196 described in Section 4 we have used the following information: the altimeter data, the modelled sea level data, the modelled wind and wave fields. Following the rules of the European Weather Centre for Medium-Range Weather Forecasts (Reading, U. K.), being their product the wind fields need to be asked to this Centre. For the two passes the directly available information are in the following files:

161–26 November 2015, 11.30 UTC.

- Altimeter data: 2015_11_26_12_total_level_profile_data_clean_161.
- Sea level profile: SHYFEM_2015_11_26_12_00.
- Wave field: HENETUS_OPE_2015_11_26_12.

196–16 November 2014, 01.30 UTC.

- Altimeter data: 2014_11_16_01_total_level_profile_data-clean_196.
- Sea level profile: SHYFEM_2014_11_16_01_30.
- Wave field: HENETUS_OPE_2014_11_16_12.

The altimeter data are a sequence of single values, identified by: sequential number, lat and lon coordinates, date (yy, mm, dd), different data. The actual sea level is the last number on the right.

The modelled sea level data are just a sequence of lon and lat coordinates plus sea level height (m).

File INFO_READ_WAVE provides the information on how to read the wave fields.

All these files are available at https://owncloud.ve.ismar.cnr.it/owncloud/index.php/s/kV3Bi9hkf9nreUj

References

Abdalla, S., Cavaleri, L., 2002. Effect of wind variability and variable air density on wave modeling. J.Geoph.Res. 107 (C7) https://doi.org/10.1029/2000JC000639, 17–1/ 17–17.

Andersen, O.B., Scharroo, R., 2011. Range and Geophysical Corrections in Coastal Regions: and Implications for Mean Sea Surface Determination, Coastal Altimetry. Springer, Berlin, Heidelberg, pp. 103–145.

Battjes, J.A., Janssen, J.P.F.M., 1978. Energy loss and set-up due to breaking of random waves, Proc. In: 16th Conf. Coastal Engineering (Hamburg), New York, ASCE, pp. 569–587.

Bertotti, L., Cavaleri, L., 2008. Analysis of the voyager storm. Ocean Eng. 35 (1), 1–5.

Bidlot, J.-R., 2019. Model upgrade improves ocean wave forecasts. ECMWF Newslett. 159.

Birol, F., Fuller, N., Lyard, F., Cancet, M., Nino, F., Delebecque, C., Fleury, S., Toublanc, F., Melet, A., Saraceno, M., Leger, F., 2017. Coastal applications from nadir altimetry: example of the X-TRACK regional products. Adv. Space Res. 59 (4), 936–953.

Birol, F., Léger, F., Passaro, M., Cazenave, A., Niño, F., Calafat, F.M., Shaw, A., Legeais, J. F., Gouzenes, Y., Schwatke, C., Benveniste, J., 2021. The X-TRACK/ALES multi-mission processing system: New advances in altimetry towards the coast. Advances in Space Research 67 (8), 2398–2415. https://doi.org/10.1016/j.asr.2021.01.049.

Boergens, E., Dettmering, D., Schwatke, C., Seitz, F., 2016. Treating the hooking effect in satellite altimetry data: a case study along the Mekong River and its tributaries. Remote Sens. 8 (2), 91,1–22. https://doi.org/10.3390/rs8020091.

Burchard, H., Petersen, O., 1999. Models of turbulence in the marine environment – a comparative study of two equation turbulence models. J. Mar. Syst. 21, 29–53.

Cavaleri, L., 2000. The oceanographic tower Acqua Alta – activity and prediction of sea states in Venice. Coast. Eng. 39, 29–70.

Cavaleri, L., Bertotti, L., 2003. The characteristics of wind and wave fields modelled with different resolutions. Q.J.R.Meteorolog.Soc. 129, 1647–1662.

Cavaleri, L., Bertotti, L., 2004. Accuracy of the modelled wind and wave fields in enclosed seas. Tellus 56A, 167–175.

Cavaleri, L., Abdalla, S., Benetazzo, A., Bertotti, L., Bidlot, J.-R., Breivik, O., Carniel, S., Jensen, R.E., Portilla-Jandun, J., Rogers, W.E., Roland, A., Sanchez-Arcilla, A., Smith, J.M., Staneva, J., Toledo, Y., van Vledder, G.Ph., van der Westhuysen, A.J.,

2018. Wave modelling in coastal and inner seas. Prog. Oceanogr. 167, 164–233. https://doi.org/10.1016/j.pocean.2018.03.010.

Cavaleri, L., Bertotti, L., Pezzutto, P., 2019a. Accuracy of altimeter data in inner and coastal seas. Ocean Sci. 15, 227–233. https://doi.org/10.5194/os-15-227-2019.

Cavaleri, L., Bajo, M., Barbariol, F., Benetazzo, A., Bertotti, L., Chiggiato, J., Davolio, S., Ferrarin, C., Magnusson, L., Papa, A., Pezzutto, P., Pomaro, A., Umgiesser, G., 2019b. The October 29, 2018 storm in northern Italy – an exceptional event and its modeling. Prog. Oceanogr. 178, 1–15.

Cipollini, P., Benveniste, J., Birol, F., Fernandes, M.J., Obligis, E., Passaro, M., et al., 2017. Satellite altimetry in coastal regions. In: Satellite Altimetry over Oceans and Land Surfaces Earth Observation of Global Changes Book Series, Eds.

Davolio, S., Stocchi, P., Benetazzo, A., Bohm, E., Riminucci, F., Ravaioli, M., Li, X.M., Carniel, S., 2015. Exceptional bora outbreak in winter 2012: validation and analysis of high-resolution atmospheric model simulations in the northern Adriatic area. Dynam. Atmos. Ocean. 71, 1–20.

Davolio, S., Henin, R., Stocchi, P., Buzzi, A., 2017. Bora wind and heavy persistent precipitation: atmospheric water balance and role of air-sea fluxes over the Adriatic Sea. Q. J. R. Meteorol. Soc. 143 (703), 1165–1177.

Donelan, M.A., Magnusson, A.-K., 2017. The making of the Andrea wave and other rogues. Sci. Rep. 7, 44124. https://doi.org/10.1038/srep44124.

ESA, 2019. Living Planet Symposium, 13–17 May 2019, Milan, Italy. https://lps19.esa.in t/NikalWebsitePortal/living-planet-symposium-2019/lps19.

Ferrarin, C., Roland, A., Bajo, M., Umgiesser, G., Cucco, A., Davolio, S., Buzzi, A., Malguzzi, P., Drofa, O., 2013. Tide-surge-wave modelling and forecasting in the Mediterranean Sea with focus on the Italian coast. Ocean Model 61, 38–48. https:// doi.org/10.1016/j.ocemod.2012.10.003.

Ferrarin, C., Bellafiore, D., Sannino, G., Bajo, M., Umgiesser, G., 2018. Tidal dynamics in the inter-connected Mediterranean, Marmara, Black and Azov seas. Prog. Oceanogr. 161, 102–115.

Holthuijsen, L.H., 2007. Waves in Oceanic and Coastal Waters. Cambridge University Press. https://doi.org/10.1017/CBO9780511618536 (387 pp).

Horsburgh, K.J., Wilson, C., 2007. Tide-surge interaction and its role in the distribution of surge residuals in the North Sea. J. Geophys. Res. Oceans 112 (8), 1–13. https:// doi.org/10.1029/2006JC004033.

Jensen, R.E., Swail, V., Bouchard, R.H., Bradshaw, B., 2017. Quantifying Wave Measurement Differences in Historical and Present Wave Buoy Systems, 15th

International Workshop on Wave Hindcasting and Forecasting, Liverpool, UK, 10–15 September 2017. http://www.waveworkshop.org.

Komen, G.J., Cavaleri, L., Donelan, M., Hasselmann, K., Hasselmann, S., Janssen, P.A.E. M., 1994. Dynamics and Modelling of Ocean Waves. Cambridge University Press (532 pp).

Lazaro, C., Fernandes, M.J., Vieira, T., Vieira, E., 2020. A coastally improved global dataset of wet troposphere corrections for satellite altimetry. Earth Syst. Sci. Data 12, 3205–3228. https://doi.org/10.5194/essd-12-3205-2020.

Longuet-Higgins, M.S., Stewart, R.W., 1964. Radiation stress in water waves: physical discussion and applications. Deep-Sea Res. 11 (4), 529–562.

Marti, F., Cazenave, A., Birol, F., Passaro, M., Leger, F., Nino, F., Almar, R., Benveniste, J., Legeais, J.F., 2019. Altimetry-Based Sea level trends along the coasts of western Africa. Adv. Space Res. https://doi.org/10.1016/j.asr.2019.05.033.

Passaro, M., Cipollini, P., Vignudelli, S., Quartly, G.D., Snaith, H.M., 2014. ALES: a multimission adaptive subwaveform retracker for coastal and open ocean altimetry. Remote Sens. Environ. 145, 173–189.

Passaro, M., Fenoglio-Marc, L., Cipollini, P., 2015. Validation of significant wave height from improved satellite altimetry in the German bight. IEEE Trans. Geosci. Remote Sens. 53 (4), 2146–2156.

Passaro, M., Dinardo, S., Quartly, G.D., Snaith, H.M., Benveniste, J., Cipollini, P., Lucas, B., 2016. Cross-calibrating ALES Envisat and CryoSat-2 delay–Doppler: a coastal altimetry study in the Indonesian seas. Adv. Space Res. 58 (3), 289–303.

Pugh, D.T., 1996. Tides, surges, and mean-sea level. J. Wiley Sons, 486 pp.

Shi, Q., Bourassa, M.A., 2019. Coupling Ocean currents and waves with wind stress over the Gulf stream. Remote Sens. 11 (12), 1476. https://doi.org/10.3390/rs11121476.

Smagorinsky, J., 1963. General circulation experiments with the primitive equations, I. the basic experiment. Mon. Weather Rev. 91, 99–152.

Stocchi, P., Davolio, S., 2017. Intense air-sea exchanges and heavy orographic precipitation over Italy: the role of Adriatic Sea surface temperature uncertainty. Atmos. Res. 196 (Supplement C), 62–82.

The ISMAR Team, Cavaleri, L., Bajo, M., Barbariol, F., Bastianini, M., Benetazzo, A., Bertotti, L., Chiggiato, J., Ferrarin, C., Trincardi, F., Umgiesser, G., 2020. The 2019 flooding of Venice and its implications for future predictions. Oceanography 33 (1), 42–49. https://doi.org/10.5670/oceanog.2020.105.

Tournadre, J., 2014. Anthropogenic pressure on the open ocean: the growth of ship traffic revealed by altimeter data analysis. Geophys. Res. Lett. 41, 7924–7932. https://doi.org/10.1002/2014GL061786.

Umgiesser, G., Ferrarin, C., Cucco, A., De Pascalis, F., Bellafiore, D., Ghezzo, M., Bajo, M., 2014. Comparative hydrodynamics of 10 Mediterranean lagoons by means of numerical modeling. J. Geophys. Res. Oceans 119, 2212–2226. https://doi.org/10.1002/2013JC009512.

Vignudelli, S., Birol, F., Benveniste, J., Fu, L.L., Picot, N., Raynal, M., Roinard, H., 2019. Satellite altimetry measurements of sea level in the coastal zone. Surv. Geophys. 40 (6), 1319–1349.

Williams, J., Horsburgh, K., Williams, J., Proctor, R., 2016. Tide and skew surge independence: new insights for flood risk. Geophys. Res. Lett. 43 (12), 6410–6417. https://doi.org/10.1002/2016GL069522.

Young, I.R., Ribal, A., 2019. Multiplatform evaluation of global trends in wind speed and wave height. Science 36 (6440), 548–552.